JOURNAL OF AGRICULTURAL AND FOOD CHEMISTRY

Fractionation of Monomeric and Polymeric Anthocyanins from Concord Grape (*Vitis labrusca* L.) Juice by Membrane Ultrafiltration

AHMAD KALBASI† AND LUIS CISNEROS-ZEVALLOS*

Department of Horticultural Sciences, Texas A&M University, College Station, Texas 77843-2133

Concord grape juice with 20% polymeric and 60% monomeric anthocyanin (Acy) forms was ultrafiltrated using polyvinylidene fluoride flat sheet membranes ranging from 10 to 1000K molecular weight cutoff (MWCO) to obtain different permeate and retentate fractions. Permeate flux, membrane resistance, Acy rejection, fouling, Acy content and composition, color properties, and antioxidant activity (AOX) were characterized. Results showed that permeate flux declined with lower MWCO, while membrane resistance increased and related exponentially with fouling. Anthocyanin membrane rejection differed for polymeric and monomeric Acy forms. Polymeric Acy increased (36−66%) and monomeric Acy decreased (12−20%) in retentate fractions with membrane pore size of <100K MWCO, while polymeric Acy decreased (11−28%) and monomeric Acy increased (5−7%) in permeate fractions. Fraction properties showed that AOX related linearly with the total phenolic content, while lightness and chroma color properties related linearly to the monomeric Acy content. These results indicate that ultrafiltration can be used to tailor monomeric and polymeric Acy fractions with potential effects in color and bioactive properties.

KEYWORDS: Grape anthocyanin composition; fractionation; ultrafiltration; color; membranes; antioxidants

INTRODUCTION

Grape juice and grape skin extracts are an important commercial source of anthocyanins (Acy). Grape juice has a high proportion of monomeric and a small amount of polymeric Acy forms (*1*). Recent work has shown evidence of oligomeric Acy in grape skin extracts (*2*). Anthocyanins exert different functional properties such as color potential, antimicrobial, antioxidant activity, and health benefits (*3*−*6*).

There are four Acy-derived food colorants used in the U.S. market including a grape skin extract, grape color extract, fruit juices, and vegetable juices that have been approved by the FDA (*7*). Among the methods used for concentration and separation of colorants, ultrafiltration (UF) technology has been used for separation of different grape Acy-based products, such as grape Acy skin extracts (*8*), red wine (*9*), and grape juice (*10*) using different types of membranes and pore size. The performance of a given membrane is dependent upon several factors including the transmembrane pressure, crossflow velocity, molecular weight cutoff (MWCO), concentration of dissolved solids, and fouling characteristics of the membrane (*8*). The MWCO is a term associated to pore size and is used to describe the potential separating capabilities of a UF membrane. It refers to the molecular weight of a solute, such as a globular protein, that is 90% rejected by the membrane under standard conditions (*11*).

Molecular masses of grape monomeric Acy pigment glycosides are ∼350−600 Da (*12*); however, commercial grape pigment extracts are highly polymerized macromolecules of ∼12000 Da, with characteristics of both Acy and tannins, and are known as anthocyanotannins (*13*). Other Acy forms, such as vitisin A (malvidin-3-*O*-glucoside pyruvic acid), vitisin B (malvidin-3-*O*-glucoside vinyl adduct), and their derivatives (including acetylvitisin A, *p*-coumaroylvisitin A, acetylvisitin B, and *p*-coumaroylvisitin B) are pigments with molecular weights in the range of 530−730 (*14*−*18*).

Since grape UF products may contain different amounts of monomeric, polymeric and other Acy forms due to differences in molecular weight, it is very likely that the relative Acy form contents will affect functional properties such as color potential and possibly antioxidant activities. Thus, the selection of the appropriate type of membrane and MWCO would influence these properties in the obtained fractions.

In the present study, we evaluated the potential use of UF for tailoring permeate and retentate Acy fractions from Concord grape juice to obtain different functional properties. In our approach, we characterized the influence of different membrane MWCO on the monomeric and polymeric Acy composition of permeates and retentates as well as their effects on color and antioxidant properties.

* To whom correspondence should be addressed. Phone: (979) 845-3244. Fax: (979) 845-0627. E-mail: lcisnero@taexgw.tamu.edu.

† Visiting Assistant Professor, Department of Food Science and Engineering, University of Tehran, Tehran, Iran.

10.1021/jf0706068 CCC: $37.00
Published on Web 08/01/2007

MATERIALS AND METHODS

Grape Juice Samples. Frozen concentrated Concord grape juice (Welch's Concord) containing 85 mg of Acy/100 g was diluted with water to obtain two initial feed concentrations of 17 and 8.5 mg of Acy/100 g of solution. The prepared samples were then centrifuged at 10 000 rpm for 1 h to remove suspended polymers such as proteins, tannins, and polysaccharide complexes in red grape juice (*19*). The clear juice was removed from each centrifuge bottle, and its precipitate was weighed giving ~0.37 and 0.30% w/w sediment and °Brix of ~10.6 and 5.2 for initial feed concentrations of 17 and 8.5 mg of Acy/100 g of solution, respectively. The °Brix remained constant for each run in the retentate and permeate fractions.

Ultrafiltration Process. Prepared samples were run through polyvinylidene fluoride (PVDF) membranes of 1000, 500, 250, 100, 30, and 10K MWCO (Niro, GEA Filtration, Hudson, WI.). PVDF is a polymer membrane widely used in the food and medicine field for ultrafiltration (*20*, *21*). A pilot plant ultrafiltration unit (model LAB-20-0.72, DDS RO- Division, Nakskov, Denmark) with four flat sheet membranes was used for each run (total membrane area, $Area_m$ = 0.122 522 4 m^2). The ultrafiltration unit operated in the mode of batch ultrafiltration with full recycle of the retentate and a transmembrane pressure (ΔP) of 400 kPa. Samples of 2 L were used for each run at room temperature until obtaining final volumes of 1.8 L of permeate and 0.2 L of retentate. Two to three replicates were used for each run.

Permeate flux was determined at room temperature by ultrafiltration of 2 L of water and for both feed solutions. Permeate flux was calculated by measuring periodically the time needed to produce 200 mL of permeate until reaching a final permeate volume of 1.8 L. The slope of the linear portion of the curve was used for estimating the flux. For membranes of 250−1000K MWCO, linear curves were obtained for collected permeate volumes of >200 mL, while for membranes of 10−100K MWCO, linear curves were obtained for collected permeate volumes of >800 mL. Membrane permeate flux (J) relates to the overall membrane resistance (R_m) by (*11*),

$$J = \Delta P/R_m \quad (1)$$

where J is defined in L/m^2·h, R_m in kPa m^2·h/L, and ΔP in kPa.

The performance of each membrane MWCO is characterized by determining the rejection factor (R) using the following expression (*22*),

$$R = 1 - C_p/C_r \quad (2)$$

where C_p and C_r are the permeate and retentate Acy concentrations, respectively, in mg/mL.

Anthocyanin and Total Phenolic Analysis. Total phenolics were quantified by the Folin−Ciocalteu method (*23*) and reported as milligrams of chlorogenic acid, while Acy content was measured by the Fuleki and Francis method (*24*) and reported as milligrams of cyanidin-3-glucoside (molecular weight 449/mol, $E = 25965\ M^{-1}\ cm^{-1}$) (*25*). The monomeric, polymeric, and other Acy form pigment content was determined using the bisulfite solution method, in which grape solutions were bleached with potassium metabisulfite and the absorbance reading (A) were taken on bleached and nonbleached samples at the Acy λ_{max}, 420 and 700 nm (*26*). In this method, the monomeric Acy are bleached by bisulfite, whereas polymeric Acy pigments are not since the number 4 position in the molecule is blocked. Similarly, other Acy forms or visitin-type pigments also have the 4 position blocked (due to formation of an additional ring by reaction with pyruvic acid or acetaldehyde) (*17*) and are not bleached with bisulfite. The different Acy forms including monomeric, polymeric, and other Acy forms were calculated as follows:

(a) monomeric Acy (%) = (monomeric color/color density) × 100 where monomeric color = ($A_{\lambda max}$ of sample − A_{700nm} of sample) − ($A_{\lambda max}$ of bleached sample − A_{700nm} of bleached sample) and color density of sample = ($A_{\lambda max} - A_{700nm}$) + ($A_{420nm} - A_{700nm}$)

(b) polymeric Acy (%) = (polymeric color/color density) × 100 where polymeric color of bleached sample = ($A_{\lambda max} - A_{700nm}$) + ($A_{420nm} - A_{700nm}$)

(c) other Acy forms (%) = 100 − (monomeric Acy (%) + polymeric Acy (%)).

Antioxidant Activity and Color Properties. Selected retentate and permeate fractions with different total phenolic and Acy content (monomers and polymers) were used for determining color properties and antioxidant activity. The antioxidant activity (AOX) was determined by the Brand-Williams et al. method (*27*). Samples from the selected retentate and permeate fractions were allowed to react with a stable radical, 2,2-diphenyl-1-picrylhydrazyl (Sigma Chemical Co., St. Louis, MO) monitoring absorbance readings at 515 nm through time until steady state. Results were expressed as micrograms of Trolox equivalent using a standard curve (*28*).

For measurements of color properties, samples from selected retentate and permeate fractions were adjusted to a similar absorbance range of 0.55−0.56 using deionized water and evaluated at 520−524 nm and pH of 3.1−3.2. Afterward, lightness (L), chroma (Ch), and hue (H) were measured with a Minolta CT-310 colorimeter (Minolta Corp., Ramsey, NJ) using a 2-mm-cell path cuvette and light source D. The L, Ch, and H values were plotted against the percent of monomer Acy present in the samples.

In general, each UF run was replicated two or three times, and all collected data were processed statistically using linear or nonlinear regression analysis with 3.08 KaleidaGraph Synergy software (Reading, PA) and 1.01 CA-CricketGraph III software (Islanadia, NY).

RESULTS AND DISCUSSION

Anthocyanin Concentration in Permeate and Retentate Fractions. Initial results showed that Acy concentration in the retentate and permeate fractions was dependent on membrane MWCO and followed a logarithmic relationship of the type

$$C_p \text{ or } C_r = K_1 + K_2\ \text{Ln(MWCO)} \quad (3)$$

where K_1 and K_2 are constants of the equation ($r^2 \sim 0.77-0.92$) (**Figure 1A**,**B**). After a 10-volume reduction of the initial feed solution, MWCO membranes of 1000K showed retentate and permeate Acy concentrations similar to that of the initial feed solution ($p > 0.05$). For membranes in the range of 1000K−30K MWCO, the retentate and permeate Acy concentrations slightly increased and decreased, respectively, and these changes were even larger for MWCO < 30K (~2-fold). This trend was observed for both initial feed Acy concentrations used (**Figure 1A**,**B**), and could be associated with the smaller membrane pore size, the possible presence of Acy deposition, and the gel layer formed, which would increase the overall resistance to Acy movement through the membrane.

Permeate flux, Membrane Resistance, and Fouling. For each membrane MWCO, plotting permeate volume versus time gave linear curves for water and nonlinear curves for the Acy solutions (**Figure 2A**,**B**). The permeate fluxes for water and the Acy solutions were calculated from the slopes using the linear portion of the curves (**Table 1**). The resulting water flux value was relatively constant for different membrane MWCO (~41.2 L/m^2·h), while for Acy solutions, it declined with membrane MWCO. Water flux value was ~2.6−11.4-fold higher than the Acy solution fluxes at the range of MWCO tested. The decline in permeate flux of the Acy solutions through time (**Figure 2A**,**B**) and for each membrane MWCO (**Table 1**) could be due to the gel layer formed, the presence of fouling, or both (*29*), affecting the overall membrane resistance.

The calculated membrane resistance, R_m (eq 1) for permeate water flux, was relatively constant at different MWCO (~9.7 kPa m^2·h/m, **Figure 3A**). However, the R_m for Acy solutions increased with decreasing membrane MWCO. For example, at a 1000K and 10K MWCO, the R_m values for Acy permeates were ~2.7 and 9.5-fold higher, respectively, compared to that of pure water. In general, the R_m values were slightly higher for the feed solution with higher initial Acy concentration.

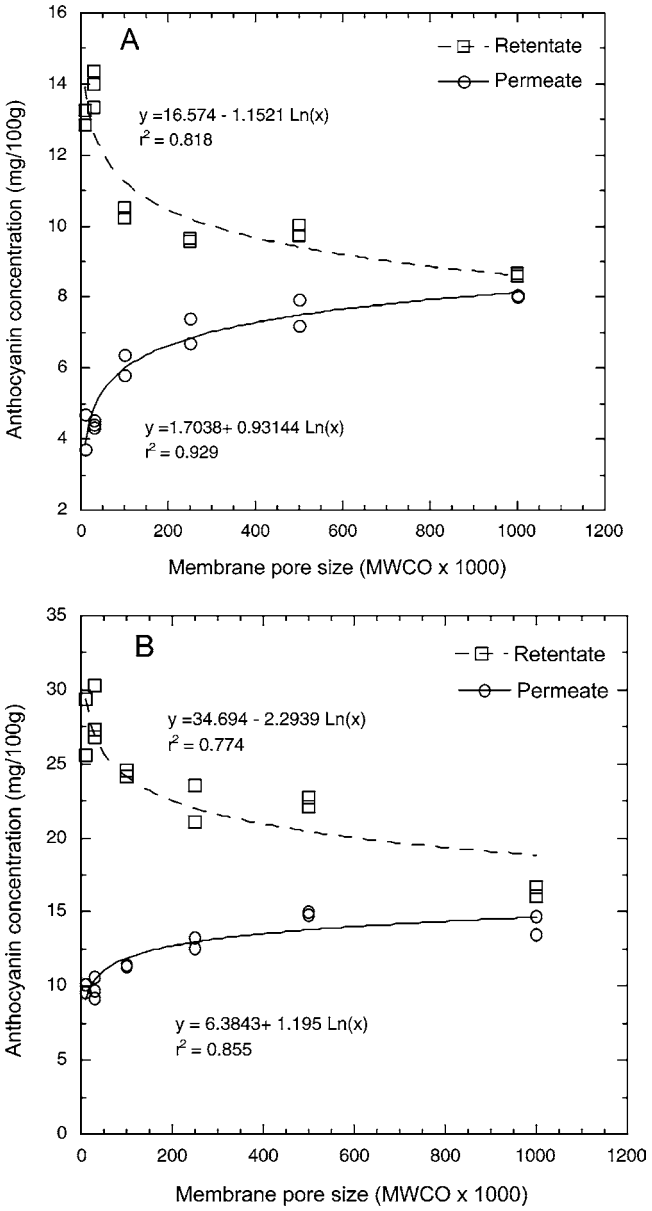

Figure 1. Effect of membrane pore size on Acy concentration of permeate and retentate fractions of grape juice with initial feed Acy concentration of (**A**) 8.5 and (**B**) 17 mg/100 g of solution, and after a 10-volume reduction of the initial feed. Solid and dotted lines correspond to eq 3.

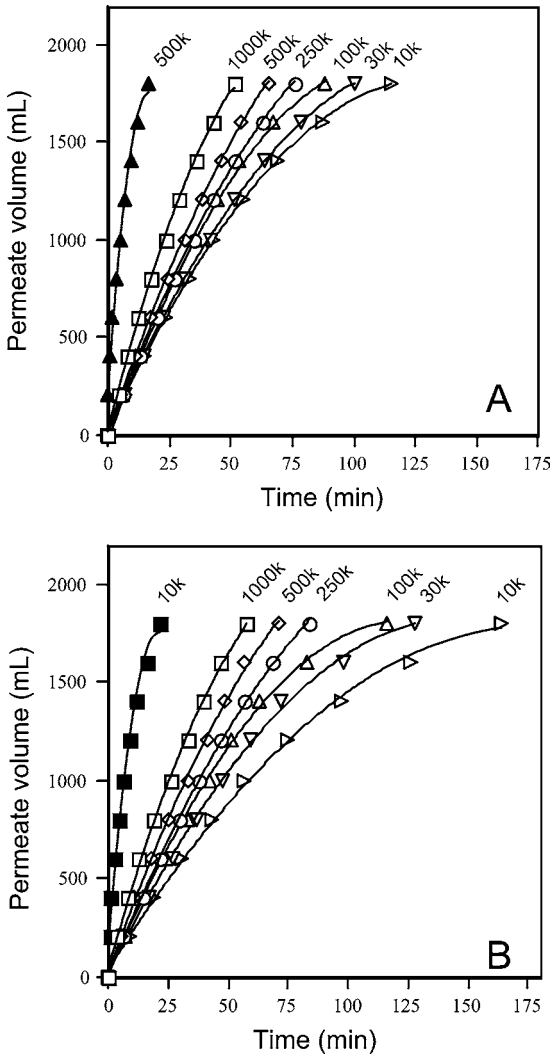

Figure 2. Permeate volume through time for water (closed symbols) and grape juice (open symbols) with initial feed Acy concentrations of (**A**) 8.5 and (**B**) 17 mg/100 g of solution.

Table 1. Estimated Permeate Flux (*J*) from the Permeate Volume versus Time Curves (**Figure 2A**,**B**)

membrane MWCO	initial feed solution (17 mg Acy/100 g) J (L/m²·h)	initial feed solution (8.5 mg Acy/100 g) J (L/m²·h)
1000K	13.82	15.7
500K	11.72	12.85
250K	10.01	10.99
100K	5.07	7.30
30K	4.69	6.58
10K	3.61	5.39

It has been reported that intrinsic membrane resistance (R'_m) relates to pore size (p) following the power relationship $R'_m \sim f(p^{-2})$ (*11*). Similarly, in the present study, R_m was related to MWCO by the power relationship

$$R_m = K_3\,(\mathrm{MWCO})^{K_4} \qquad (4)$$

where K_3 and K_4 are constants of the equation. Using eq 4 gave curves with good visual fitting and an $r^2 > 0.91$ (**Figure 3A**). The obtained K_3 and K_4 values were 136.63 kPa m²·h/L and −0.236, respectively, for an initial feed Acy concentration of 8.5 mg/100 g, and 246.36 kPa m²·h/L and −0.309, respectively, for an initial feed Acy concentration of 17 mg/100 g. The lower power values obtained for K_4 using MWCO compared to p would depend most likely on the specific relationship existent between MWCO and the membrane pore size (p).

The overall membrane resistance R_m is formed by the intrinsic membrane resistance R'_m, the fouling resistance R_f, and the gel layer resistance R_g (*11*); thus, $R_m = R'_m + R_f + R_g$. The R'_m was already estimated using water flux in the present study. The R_f would depend on the Acy deposition on the membrane or fouling (i.e., anthocyanin−membrane interactions) while R_g would depend on parameters that affect the gel layer formation including pressure, feed concentration, and feed velocity (*11*).

After each batch run of an Acy solution, membranes had the presence of Acy deposition. The amount of Acy membrane deposition (Acy_m) was determined for each pore size using the experimental data of Acy concentrations, C_o, C_r,

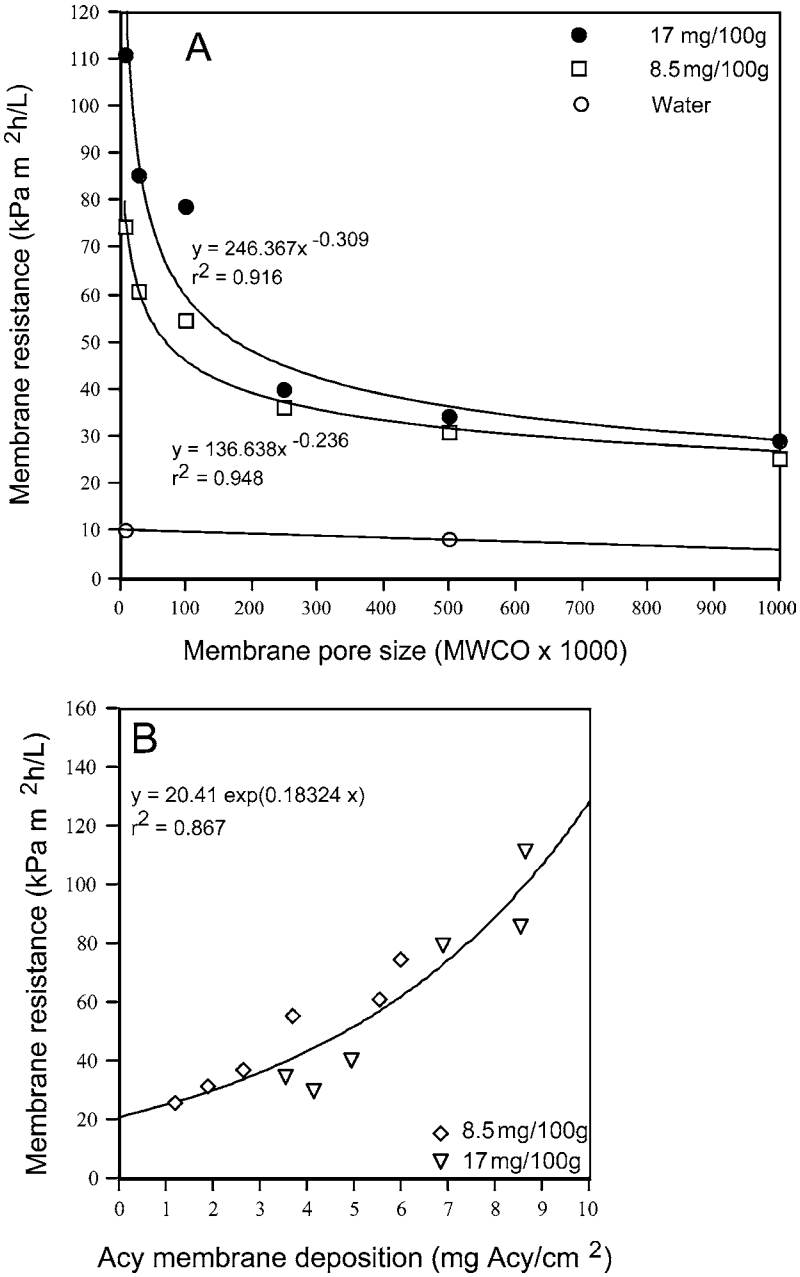

Figure 3. Relationship between overall membrane resistance (R_m) and (**A**) membrane pore size and (**B**) membrane anthocyainin deposition (Acy_m/$Area_m$), for grape juice samples. Solid lines of power curves in (**A**) correspond to eq 4 and solid line in (**B**) correspond to eq 6.

and C_p, the corresponding volumes and a mass balance. Thus,

$$Acy_m = C_o V_o - C_r V_r - C_p V_p \quad (5)$$

where C_o is initial feed Acy concentration (mg/mL) and V_o, V_r, and V_p are the initial feed, retentate, and permeate volumes (mL), respectively. The calculated Acy membrane deposition expressed as $Acy_m/Area_m$ (mg/m^2) ranged from ~1.2 to 6 for an initial feed Acy concentration of 8.5 mg/100 g and from ~3.5 to 8.6 for an initial feed Acy concentrations of 17 mg/100 g.

Results indicated that the overall membrane resistance increased with increasing amounts of Acy membrane deposition or fouling, for both initial feed Acy concentrations used (**Figure 3B**). Plotting R_m versus $Acy_m/Area_m$ gave a distinct exponential relationship of the type

$$R_m = K_5 \exp(K_6 Acy_m/Area_m) \quad (6)$$

where K_5 and K_6 are constants (r^2~ 0.86). Equation 6 was obtained by inserting C_r and C_p described by eq 3 and by inserting R_m described by eq 4, into the anthocyanin mass balance described by eq 5. The curve intersected the Y axis (constant K_5) at a value of ~20.4 kPa m^2·h/L corresponding to the resistance $R'_m + R_g$ (assuming that R_g is constant for each pore size and independent of $Acy_m/Area_m$ values). Resistance values above the intersection in the Y axis would correspond solely to the fouling resistance, R_f, which would be dependent on the $Acy_m/Area_m$ values.

According to these results, since R'_m was ~ 9.7 kPa m^2·h/L (**Figure 3A**), then R_g was ~10.7 kPa m^2·h/L for both feed solutions used. On the other hand, R_f ranged from ~5 to 53.7 and from ~8.5 to 90.2 kPa m^2·h/L for initial feed Acy concentrations of 8.5 and 17 mg/100 g, respectively. Thus, the contribution of individual resistances followed the order $R_f >> R_g \geq R'_m$. The R_f played a major role in increasing the overall

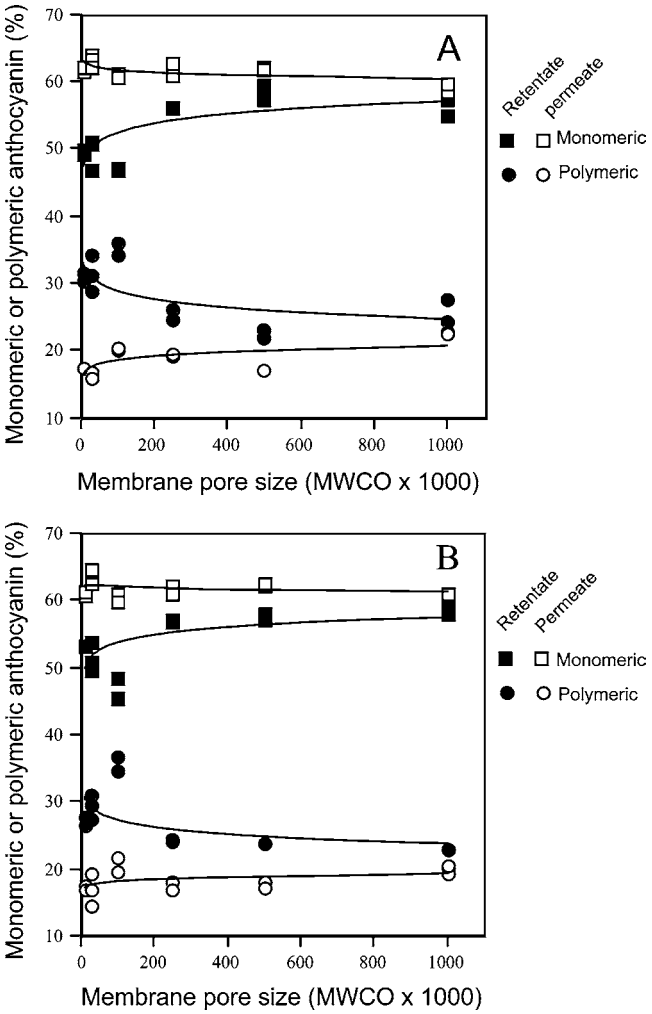

Figure 4. Membrane pore size effects on monomeric and polymeric Acy composition of permeate and retentate fractions using initial feed Acy concentrations of (**A**) 8.5 and (**B**) 17 mg/100 g of solution. Solid lines correspond to eq 3.

membrane resistance to permeate flux especially at smaller membrane MWCO (**Figure 3B**).

The presence of an exponential relationship instead of a linear curve for both initial feed Acy concentrations suggests that Acy fouling followed different particle deposition patterns, which affected the overall membrane resistance. Membrane fouling may occur by deposition of particles inside the pores or on top of the pore membrane (*30*). These deposition patterns would have differing effects on membrane resistance. According to this, it is likely that, for an initial Acy feed of 8.5 mg/100 g, fouling was caused mainly by deposition of particles inside the pores and in smaller proportion on top deposition, while for an initial Acy feed of 17 mg/100 g, fouling occurred by a combination of particle deposition inside pores and a larger proportion of deposition on top.

Anthocyanin Fractionation and Rejection. The grape Acy's used in this study were formed by ∼60% monomers, ∼20% polymers, and ∼20% of other Acy forms. This composition was similar for both initial Acy feed solutions used. After a 10-volume reduction in the UF process, the Acy composition of retentate and permeate fractions differed from the initial feed for each membrane MWCO (**Figure 4A**,**B**) with a larger effect for MWCO < 100K. For example, permeate had higher monomer (5−7%) and lower polymer Acy content (11−28%) compared to the initial feed composition. On the other hand, retentate showed a lower monomer (12−20%) and higher polymer Acy content (36−66%). Other Acy forms showed changes of less than 10% with decreasing MWCO. These results indicate that different Acy fractions may be obtained using different membrane pore size. The percentage of different Acy forms followed logarithmic relationships with membrane MWCO similar to eq 3 (**Figure 4A**,**B**). Furthermore, the concentrations of different Acy forms followed logarithmic relationships with membrane MWCO as well, similar to eq 3 (data not shown).

Membrane rejections ($R_{\text{Acy form}}$) for monomer, polymer, and other Acy forms were obtained modifying eq 2 as follows,

$$R_{\text{Acy form}} = 1 - C_p(\%\text{Acy}_{\text{form}})/C_r(\%\text{Acy}_{\text{form}}) \qquad (7)$$

where ($\%\text{Acy}_{\text{form}}$) is the percent anthocyanin form corresponding to monomer, polymer, or other Acy forms.

The calculated membrane rejections showed similar curves for monomer Acy's and other Acy forms, while a higher rejection curve was observed for polymer Acy's (**Figure 5A**, **B**). For all three curves, rejection increased with decreasing MWCO. This trend was observed for both initial Acy feed solutions. The difference between rejection curves was evident in all the MWCO range tested. The obtained $R_{\text{Acy form}}$ expressed as percentage followed a nonlinear relationship with the membrane MWCO giving curves of the type

$$R_{\text{Acy form}} = 100 - (K_7 + K_8 \,\text{Ln MWCO})/(K_9 + K_{10} \,\text{Ln MWCO}) \quad (8)$$

The equation was obtained by inserting eq 3 into eq 7, where K_7−K_{10} are constants ($r^2 \sim 0.94$−0.97).

The similar rejection pattern between monomer Acy and other Acy forms would be related to their similar molecular weights. Monomer Acy have been reported to be in the range of ∼350−600 Da (*12*), while other monomeric Acy forms such as visitin-type pigments are in the range 530−730 Da (*14*−*18*). The higher rejection of polymers Acy would be related to their higher molecular masses of ∼1000−12000 Da (*2*, *13*). Overall, the three Acy forms were rejected in a broad range of membrane MWCO used despite the smaller molecule size of the Acy forms. It is likely that pore size restriction due to fouling, the presence of association within each Acy form (e.g., hydrogen bonding), or both factors together influenced rejection. Nevertheless, differences in molecular weight among the Acy components and the use of a range of membrane pore size confirm the potential for tailoring different Acy fraction compositions using membrane technology.

Fraction Properties. In this part of the study, we characterized the color properties of different retentate and permeate Acy fractions obtained with membranes of 30K MWCO from both initial feed Acy solutions and adjusted to similar absorbance (∼0.55). Results showed that *L* and Ch increased linearly with increasing percentage of monomer Acy ($r^2 > 0.96$), while not affecting *H* values (**Figure 6**). Adjusting the composition of monomeric Acys indicates the potential of tailoring fractions with differing color attribute intensities.

In addition, we characterized the antioxidant or antiradical activities (AOX) of retentate and permeate fractions obtained with membranes of 30K MWCO and the two initial feed Acy solutions (**Figure 7**). Results showed a linear relationship between total phenolics present in each fraction and AOX ($r^2 \sim 0.99$). Fractions with higher phenolic content (mg/mL) showed higher antioxidant activity (μg of trolox/mL) as expected. The slope of the linear relationship indicated that the total phenolic compounds present in each fraction analyzed had

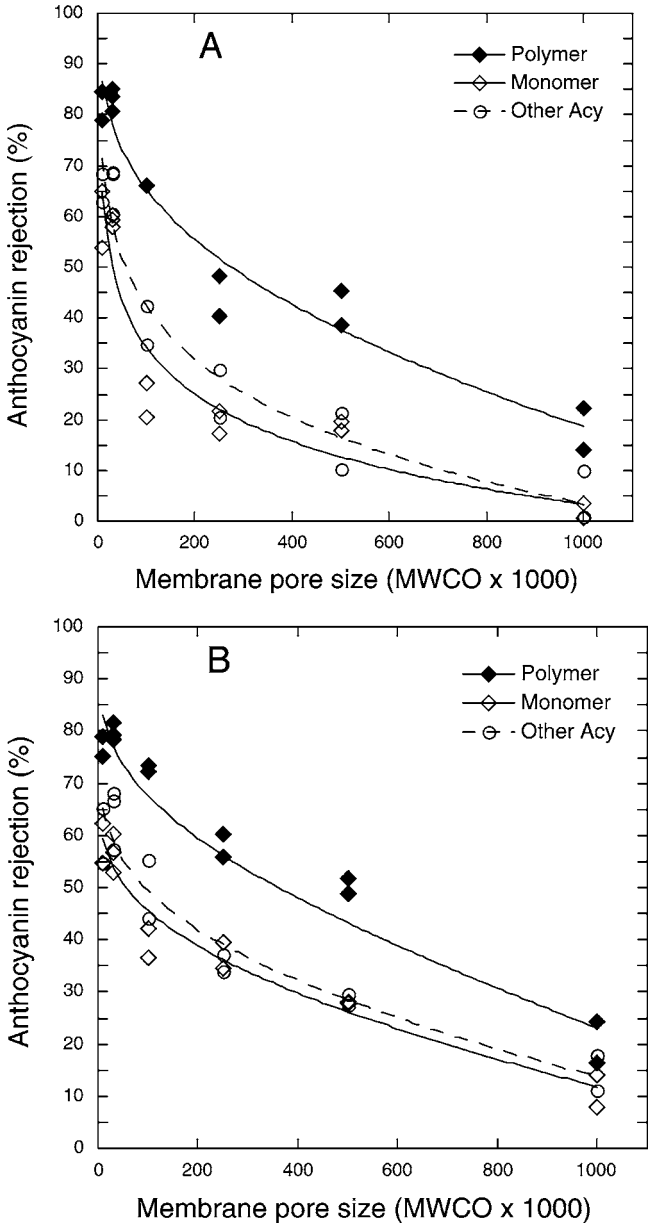

Figure 5. Membrane pore size effects on rejection (*R*) of monomeric, polymeric, and other Acy forms of grape juice samples with initial feed Acy concentrations of (**A**) 8.5 and (**B**) 17 mg/100 g of solution. Solid and dotted lines correspond to eq 8.

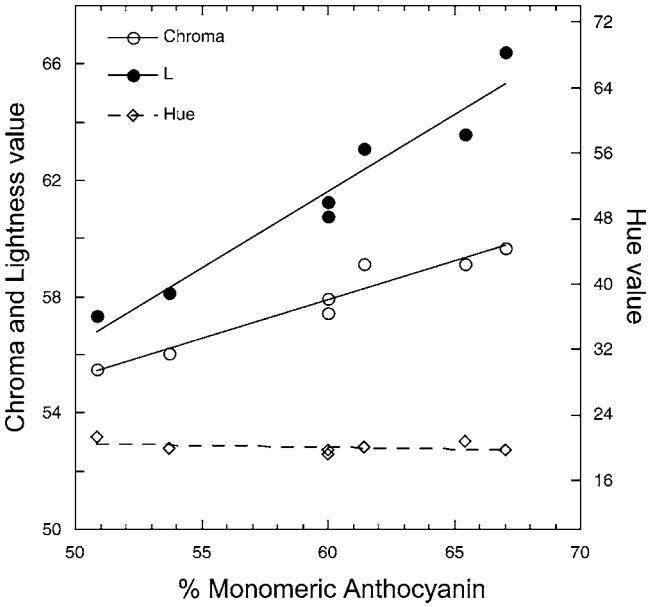

Figure 6. Monomeric Acy composition effects on color parameters, Hue, chroma, and lightness, using different permeate and retentate fractions obtained with 30K MWCO membranes and standardized to an Acy absorbance of 0.55 measured at 520–524 nm and pH 3.1–3.2.

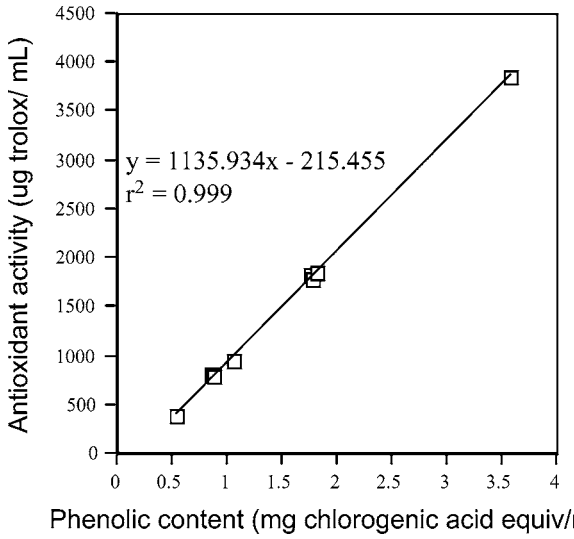

Figure 7. Antioxidant activity of different permeate and retentate fractions with differing total phenolic content.

similar antiradical properties on a phenolic basis (~1135 μg of trolox/mg of phenolic). These results suggest that despite each fraction showing different polymer and monomer Acy compositions, it did not affect the antioxidant activity on a phenolic basis. It is likely that since the Acy content represented only ~6−9% of the total phenolic content of each fraction used, it did not affect the scavenging properties of other phenolic compounds present in larger proportion. In the present study, total phenolic and Acy content ranged from ~54 to 359 mg of CHA/100 mL and from ~3.3 to 26.8 mg of Acy/100 mg of solution, respectively. Concord grape main phenolic groups include benzoic acids, hydroxy cinnamates, anthocyanins, flavan-3-ols, and flavonols (*31*). In general, the relatively small amount of Acy in the obtained fractions affected only color properties but was not enough to affect the antioxidant activity on a phenolic basis.

According to these results, processing extracts from crops with initial relative higher levels of Acy in relation to total phenolics (e.g., 47−48% Acy for blueberries (*28*), 77% Acy for purple corn (*32*)) would be important to obtain the full benefit of membrane technology for Acy fractionation and its use in bioactive properties. However, crops with relative lower levels of Acy would be more limiting (e.g., 14−16% Acy for Concord grape (*33*), 19% Acy for sweet potato, (*28*)). In addition, strategies that could increase the relative amount of Acy in relation to the total phenolics before UF processing would be useful, such as ion-exchange columns and liquid−liquid separation among other methods. Sequential membrane pore size UF would be an interesting approach to be considered for Acy fractionation. Previous work with olive phenols using a sequential membrane fractionation approach was shown to be very promising for testing bioactive properties (*34*).

In general, a mixture of different Acy forms is present usually in plant extracts, and the bioactivity and functionality are tested that way. However, recent work by Tsai et al. (*35*) has shown that antioxidant properties depend on the Acy form. The present

study has demonstrated that membrane technology could be used for tailoring monomer and polymer Acy fractions. The simple empirical equations proposed in this study may be used for this purpose. The Acy composition of the fractions may affect color properties and could potentially influence other functional properties as well, including antioxidant activity.

LITERATURE CITED

(1) Hong, V.; Wrolstad, R. Characterization of anthocyanin containing colorants and fruit juices by HPLC/photodiode array detection. *J. Agric. Food Chem.* **1990**, *38*, 698−708.

(2) Vidal, S.; Meudec, E.; Cheynier, V.; Skouroumounis, G.; Hayasaka, Y. Mass Spectrometric evidence for the existence of oligomeric anthocyanins in grape skins. *J. Agric. Food Chem.* **2004**, *52*, 7144−7151.

(3) Giusti, M.; Wrolstad, R. Radish anthocyanin extract as a natural red colorant for maraschino cherries. *J. Food Sci*. **1999**, *61*, 688−694.

(4) Kalt, W.; Foney, C.; Martin, A.; Prior, R. Antioxidant capacity, vitamin C, phenolics and anthocyanins after fresh storage of small fruits. *J. Agric. Food Chem*. **1999**, *47*, 4638−4644.

(5) Cevallos-Casals, B.; Byrne, D.; Okie, W.; Cisneros-Zevallos, L. Selecting new peach and plum genotypes rich in phenolic compounds and enhanced functional properties. *Food Chem*. **2006**, *96*, 273−280.

(6) Velioglu, Y.; Mazza, G.; Gao, L.; Oomah, B. Antioxidant activity and total phenolics in selected fruits, vegetables, and grain products. *J. Agric. Food Chem.* **1998**, *46*, 4113−4117.

(7) Wrolstad, R. Anthocyanins. In *Natural Food Colorants. Sciences and Technology*; Lauro, G. J., Francis, F. J., Eds.; Marcel Dekker, Inc.: New York, 2000; Chapter 11, pp 237−252.

(8) Philip, T. Purification and concentration of natural colorants by membranes. *Food Technol.* **1984**, *38* (12), 107−108.

(9) Avakyants, S. P.; Cherepin, S. A. Effect of ultrafiltration on polyphenol complexes in red table wines. *Izv. Vyssh. Uchebn. Zaved., Pishch. Tekhnol.* **1987**, *1*, 121−123.

(10) Wang, J.; Zhang, Z. D.; Liu, C. L.; Xu, L. Q. Extraction of pigments during processing of red grape juice and their physicochemical properties. *Food-Sci.,-China* **1997**, *18* (2), 32−35.

(11) Cheryan, M. In *Ultrafiltration and Microfiltration Handbook*; Technomic Publishing Co. Inc.: Lancaster, PA, 1998; pp 89, 90, 104, 116, 132, 133.

(12) Woo, A. H.; Von Elbe, J. H.; Amundson, C. H. Anthocyanin recovery from cranberry pulp wastes by membrane technology. *J. Food Sci.* **1980**, *45*, 875−879.

(13) Lin, R. I.; Hilton, B. W. Purification of commercial grape pigment. *J. Food Sci.* **1980,** *45* (2), 297−306, 309.

(14) Bakker, J. A.; Bridle, P.; Honda, T.; Kuxvano, H.; Saito, N.; Terahara, N.; Timberlakell, C. F. Identification of an anthocyanin occurring in some red wines. *Phytochemistry* **1997**, *44* (7), 1375−1382.

(15) McDougall, G. L.; Fyffe, S.; Dobson, P.; Stewart, D. Anthocyanins from red wine−their stability under simulated gastrointestinal digestion. *Phytochemistry* **2005**, *66*, 2540−2548.

(16) Asenstorfer, R. S.; Lee, D. F.; Jones, G. P. Influence of structure on the ionisation constants of anthocyanin and anthocyanin-like wine pigments. *Anal. Chim. Acta* **2006**, *563*, 10−14.

(17) Morata, A.; Calderon, F.; Gonzalez, M. C.; Gomez-Cordoves, M. C.; Suarez, J. A. Formation of the highly stable pyranoanthocyanins (vitisins A and B) in red wines by the addition of pyruvic acid and acetaldehyde. *Food Chem*. **2007**, *100*, 1144−1152. www.elsevier.com/locate/foodchem.

(18) Morata, A.; Gomez-Cordoves, M. C.; Calderon, F.; Suarez, J. A. Effects of pH, temperature and SO_2 on the formation pyranoanthocyanins during red wine fermentation with two species of *Saccharomyces*. *Int. J. Food Microbiol.* **2006**, *106*, 123−129.

(19) Fukui, M.; Yokotsuka, K. Content and origin of protein in white and red wines: changes during fermentation and maturation. *Am. J. Enol. Vitic.* **2003**, *54* (3), 178−188.

(20) Laroche, G.; Marois, Y.; Guidoin, R.; King, M. W.; Martin, L.; How, T.; Douville, Y. Polyvinylidene fluoride (PVDF) as a biomaterial: from polymeric raw material to monofilament vascular suture. *J. Biomed. Mater. Res.* **1995**, *29*, 1525−1536.

(21) Xu, Z.; Li, L.; Wu, F.; Tan, S.; Zhang, Z. The application of the modified PVDF ultrafiltration membranes in further purification of *Gingko biloba* extraction. *J. Membr. Sci.* **2005**, *255*, 125−131.

(22) Peri, C.; Riva, M.; Decio, P. Crossflow membrane filtration of wines: comparison of performance of ultrafiltration, microfiltration and intermediate cut-off membranes. *Am. J. Vitic.* **1988**, *39*, 162−168.

(23) Swain, T.; Hillis, W. E. The phenolic constituents of *Prunus domestica*. I. The quantitative analysis of phenolic constituents. *J. Sci. Food Agric.* **1959**, *10*, 63−68.

(24) Fuleki, T.; Francis, F. Quantitative methods for anthocyanins. 1. Extraction and determination of total anthocyanins in cranberries. *J. Food Sci.* **1968**, *33*, 72−77.

(25) Abdel-Aal, E. S. M.; Hucl, P. A rapid method for quantifying total anthocyanins in blue aleurone and purple pericarp wheats. *Cereal Chem.* **1999**, *76*, 350−354.

(26) Wrolstad, R. *Color and pigment analyses in fruit products*; Oregon Agriculture Experimental Station, Corvallis, OR, 1976; Bull. 624.

(27) Brand-Williams, W.; Cuvelier, M. E.; Berset, C. Use of a free radical method to evaluate antioxidant activity. *Lebensm. Wiss. Technol.* **1995**, *28*, 25−30.

(28) Cevallos-Casals, B.; Cisneros-Zevallos, L. Stoichiometric and kinetic studies of phenolic antioxidants from Andean purple corn and red-fleshed sweet potato. *J. Agric. Food Chem.* **2003**, *51*, 3313−3319.

(29) Kim, K. J.; Fane, A.; Fell, C.; Joy, D. Fouling mechanisms of membranes during protein ultrafiltration. *J. Membr. Sci.* **1992**, *68*, 79−91.

(30) Bolton, G.; LaCasse, D.; Kuriyel, R. Combined models of membrane fouling: Development and application to microfiltration and ultrafiltration of biological fluids. *J. Membr. Sci.* **2004**, *277*, 75−84.

(31) Frankel, E. N.; Bosanek, C. A.; Meyer, A. S.; Siliman, K.; Kirk, L. L. Commercial grape juices inhibit in vitro oxidation of human low-density lipoprotein. *J. Agric. Food Chem.* **1998**, *46*, 834−838.

(32) Pedreschi, R.; Cisneros-Zevallos, L. Phenolic profiles of Andean purple corn (*Zea mays* L.). *Food Chem.* **2007**, *100*, 956−963.

(33) Shukitt-Hale, B.; Carey, A.; Simon, L.; Mark, D.; Joseph, J. Effects of Concord grape juice on cognitive and motor deficits in aging. *Nutrition* **2006**, *22*, 295−302.

(34) Fiorentino, A.; Gentili, A.; Isidori, M.; Monaco, P.; Nardelli, A.; Parrella, A.; Temusi, F. Environmental effects caused by olives mill wastewaters: Toxicity comparison of low-molecular-weight phenol components. *J. Agric. Food Chem.* **2003**, *51*, 1005−1009.

(35) Tsai, P. J.; Huang, H. P.; Huang, T. C. Relationship between anthocyanin patterns and antioxidant capacity in mulberry wine during storage. *J. Food Qual.* **2004**, *27* (6), 497−505.

Received for review March 2, 2007. Revised manuscript received May 25, 2007. Accepted June 17, 2007.

JF0706068